


The following article appeared in Hydrological Processes 31(13): 2365-2380 (2017); and may be found at: <https://doi.org/10.1002/hyp.11182>

This is an open access article under the Creative Commons Attribution 4.0 International (CC BY 4.0) license
<https://creativecommons.org/licenses/by/4.0/>

RESEARCH ARTICLE

Understanding the dynamics and contamination of an urban aquifer system using groundwater age (^{14}C , ^3H , CFCs) and chemistry

Jürgen Mahlknecht¹  | Arturo Hernández-Antonio¹ | Christopher J. Eastoe² | Carol Tamez-Meléndez¹ | Rogelio Ledesma-Ruiz¹ | José A. Ramos-Leal³ | Nancy Ornelas-Soto¹

¹Centro del Agua para América Latina y el Caribe, Tecnológico de Monterrey, Monterrey, NL, Mexico

²Department of Geosciences, University of Arizona, Tucson, AZ, USA

³División de Geociencias Aplicadas, Instituto Potosino de Investigación Científica y Tecnológica, San Luis Potosí, SLP, Mexico

Correspondence

Jürgen Mahlknecht, Centro del Agua para América Latina y el Caribe, Tecnológico de Monterrey, Ave. Eugenio Garza Sada 2501, Monterrey, NL 64849, Mexico. Arturo Hernández Antonio, Centro del Agua para América Latina y el Caribe, Tecnológico de Monterrey, Ave. Eugenio Garza Sada 2501, Monterrey, NL 64849, Mexico.
Email: jurgen@itesm.mx

Funding information

Fundación FEMSA

Abstract

The quality of the groundwater supplying drinking water to the Guadalajara metropolitan area has deteriorated due to both endogenic and exogenic processes. Previous studies of this complex neotectonic volcanic environment suggest that the sources of contamination here are underground fluids derived from an active volcanic center and surface wastewater derived from regional land-use intensification. This study uses isotopic, gaseous, and chemical signatures to more comprehensively characterize this groundwater flow and its contamination paths. Groundwater is mainly recharged at the La Primavera Caldera to the west and is discharged into the Santiago River to the east. The exception to this trend is the Toluquilla area, where groundwater most likely represents rainfall originating from outside the basin limits. Evaporation affects groundwater in these areas, especially waters that have been affected by recycling below urban areas in the Atejamac area and by intensive agricultural activity in the Toluquilla area. Additionally, we present evidence that groundwater flow through alluvial sediments and tuffs in deeper wells mixes with a lower aquifer unit in basaltic-andesitic rocks, which are in contact with hydrothermal fluids. Groundwater ages range from postbomb in the western and northwestern regions of the study area (i.e., the Atemajac aquifer unit) to Late Pleistocene in the southern and southeastern regions (i.e., the Toluquilla aquifer unit). Recently recharged water records little mixing and is located mostly in or near the La Primavera volcanic system. As groundwater undergoes gravitational flow towards discharge areas, it mixes with older water components. Chloride and sodium concentrations above natural background levels are primarily related to volcanic activity, nitrate is associated with human activities, and sulfate originates from both anthropogenic sources and water–rock interactions. Nitrate originating from land-use activities (such as sewers, septic tanks, landfills, and agricultural fields) that is introduced into the deeper part of the groundwater system is expected to travel with the groundwater to the discharge areas because oxidizing conditions will prevent microbial reduction.

See Supplementary Information.

KEYWORDS

chlorofluorocarbons, environmental tracers, groundwater contamination, groundwater flow, Guadalajara, radiocarbon

This is an open access article under the terms of the Creative Commons Attribution License, which permits use, distribution and reproduction in any medium, provided the original work is properly cited.

© 2017 The Authors. Hydrological Processes Published by John Wiley & Sons Ltd.

1 | INTRODUCTION

The determination of groundwater age is fundamental to most groundwater issues. This groundwater age represents the transit time of water through a catchment and is therefore a useful parameter for describing catchment processes, such as rainfall response, streamflow generation, and sources and rates of recharge (Cartwright & Morgenstern, 2012; Mahlknecht, Gárfias-Solis, Aravena, & Tesch, 2006a; Stewart, Morgenstern, & McDonnell, 2010). The groundwater age allows workers to identify and distinguish the impacts of anthropogenic and geological contamination and is necessary for understanding the dynamics of groundwater flow and contaminant transport (Harvey et al., 2006; Horst, Mahlknecht, Merkel, Aravena, & Ramos-Arroyo, 2008; Morgenstern & Daughney, 2012; Morgenstern et al., 2015). Determining groundwater age also provides important information for assessing an aquifer's vulnerability to contamination (Eberts, Böhlke, Kauffman, & Jurgens, 2012; Mahlknecht, Medina-Mejía, Gárfias-Solis, & Cano-Aguilera, 2006b; Plummer et al., 2008). Thus, knowledge of a catchment's groundwater age may help to improve water security and can be used to manage water resources (Böhlke, Jurgens, Uselmann,

& Eberts, 2014; Broers, 2004; Kazemi, Lehr, & Perrochet, 2006; Mahlknecht, Horst, Hernández-Limón, & Aravena, 2008).

Ideally, the groundwater age of a sample represents the transit time of a water parcel in an aquifer system from an inlet (recharge area) to an exit (e.g., a well or spring). This may apply to short-screen tube wells or confined aquifers, where the groundwater recharge area is small relative to its distance from the exit (Małozewski & Zuber, 1982). However, it must be emphasized that groundwater can undergo hydrodynamic dispersion or mixing in many aquifer configurations. Therefore, the measured groundwater age in a particular well or spring typically represents a combination of different groundwater ages within the aquifer. This may be the case in catchments with a large recharge area and/or long-screen tube wells, where stratification of the groundwater age is often present (Appelo & Postma, 2005; Morgenstern et al., 2015; Zuber et al., 2005).

There is compelling evidence that the groundwater below the Guadalajara metropolitan area has been increasingly impaired for drinking water purposes as a consequence of both natural and anthropogenic processes (IMTA, 1992; SIAPA, 2004). The magma chamber below La Primavera Caldera generates hydrothermally active systems

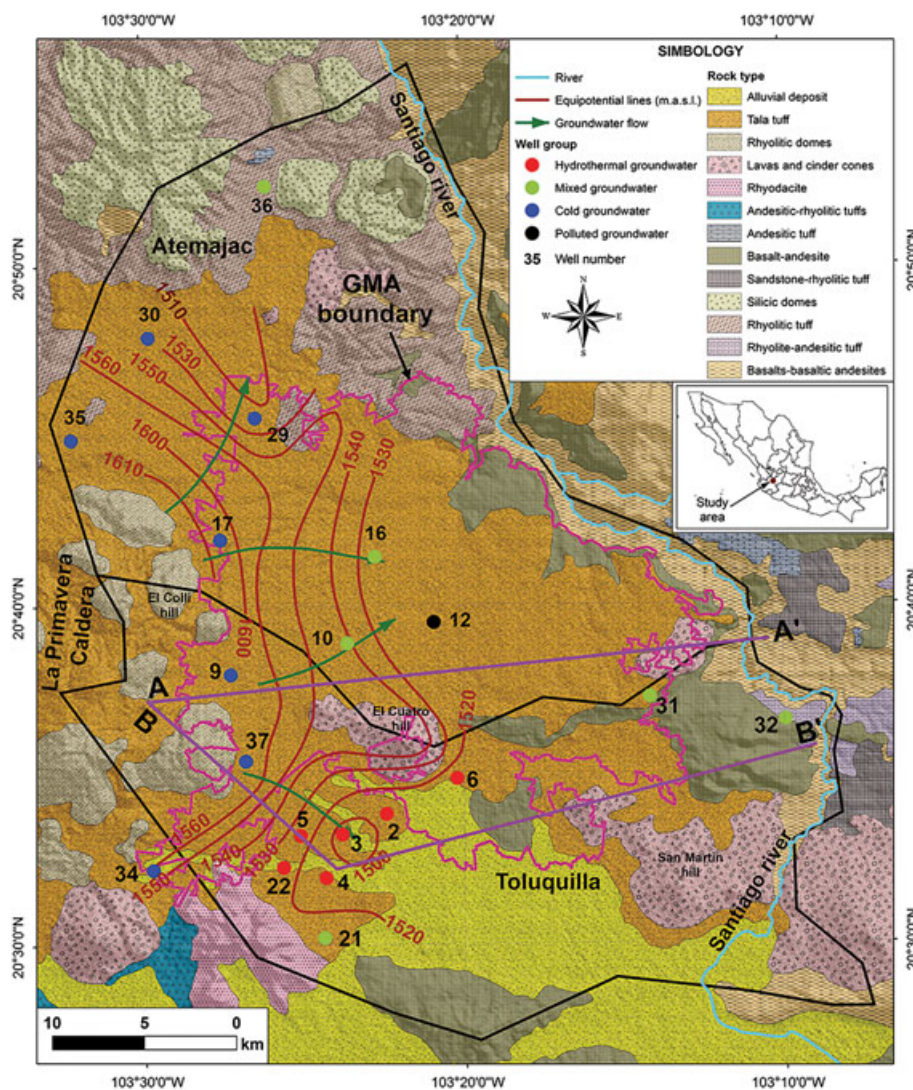


FIGURE 1 Location of study area in Mexico (box), surface geology, water table distribution, locations of wells sampled in the study area, and sections displayed in Figure 2. GMA = Guadalajara metropolitan area. Black line indicates the delimitation of the Atemajac and Toluquilla aquifer units

that are responsible for the vertical upward movement of hydrothermal fluids through faults, which then mix with regional groundwater that may undergo recharge outside of the border of the basin (Hernández-Antonio et al., 2015; Sánchez-Díaz, 2007). This groundwater circulates through basaltic and andesitic rocks, forming the deeper Atemajac–Toluquilla aquifer unit below the Toluquilla Valley (Figure 1). It is characterized by elevated temperatures, salinity, and Cl, Na, and HCO_3 contents, and contains Li, Mn, B, and F. However, exogenic groundwater pollution occurs mainly from the infiltration of runoff and sewage effluents throughout the urban area of Guadalajara, as well as from return flow from agricultural fields in the Toluquilla Valley (Hernández-Antonio et al., 2015; SIAPA, 2004). These waters are characterized by their low temperatures, variable salinity, and high concentrations of NO_3 and SO_4 , as well as by their elevated concentrations of Cl and Na.

Guadalajara's aquifer is a typical complex groundwater system, featuring a relatively deep water table (up to 150 m below ground level) and vertical flows that preclude the use of a simple flow model. However, relatively little information is available about its hydrogeological settings, well constructions, and water table configuration. Preferential groundwater flow may also account for additional local groundwater discharge (Hernández-Antonio et al., 2015). Thus, we propose an appropriate method for evaluating groundwater age distribution in order to evaluate the flow dynamics and contamination in this region.

Three-dimensional distributed-parameter groundwater-flow models with particle tracking have been successfully used by numerous investigators to anticipate the effects of non-point-source contaminant loading at the water table on production wells (Eberts et al., 2012; Kauffman, Baehr, Ayers, & Stackelberg, 2001; McMahon et al., 2008). However, these methods are generally expensive and time-consuming. As a cost-effective alternative, we propose a lumped-parameter model (LPM) coupled with tracer input functions and measured concentrations (Maloszewski & Zuber, 1996; Morgenstern et al., 2015; Zuber, 1986). LPMs are based on simplified aquifer geometries and flow configurations and may account for the effects of mixing and dispersion in the aquifer and at the borehole well. They relate the tracer concentration measured in a sample to the history of the tracer input in recharge to the aquifer (Jurgens, Böhlke, & Eberts, 2012).

Numerous studies have used isotopes and gaseous tracers in combination with LPMs in complex groundwater systems around the world to monitor the security of the global drinking water supply (e.g., Darling, Morris, Stuart, & Goody, 2005; Eberts et al., 2012; Jurgens, Böhlke, Kauffman, Belitz, & Esser, 2016; Morgenstern et al., 2015; Morris, Stuart, Darling, & Goody, 2005; Plummer et al., 2008; Turnadge & Smerdon, 2014). To date, however, only a few of these studies have been implemented in Mexico, using simplified LPMs such as piston flows or exponential mixtures (e.g., Horst et al., 2008; Mahlknecht et al., 2006a, 2008).

Tritium and chlorofluorocarbons (CFCs) are environmental pulse tracers derived from the atmosphere that are used as dating tools of young water (i.e., on timescales of 50 years or less; Cook & Solomon, 1997; Newman et al., 2010). Dating of these tracers is based on knowledge of the local input function and the measured concentration of tritium in the groundwater. The tritium concentration in the atmosphere—and thus in young groundwater—recently decreased in North

America from its maximum value at the bomb-tritium peak of the 1960s, ultimately reaching prebomb values around 1992 (Eastoe, Watts, Ploughe, & Wright, 2012). Horst et al. (2008) estimated the local input function of tritium in an area near Guadalajara using International Atomic Energy Agency/Global Network of Isotope in Precipitation data from its two closest stations (Chihuahua and Veracruz). In contrast, the historical atmospheric concentration of CFCs—and thus the air-mixing ratios recorded in groundwater—is very well documented (Clark & Fritz, 1997; Cook & Solomon, 1997; Kendall & McDonnell, 2012; Leibundgut, Maloszewski, & Külls, 2009).

Radiocarbon (^{14}C) is the leading tool for estimating the age of paleo- and fossil groundwater, which can be used to date samples that are hundreds of years to approximately 35,000 years old (Clark & Fritz, 1997; Li et al., 2015). Radiocarbon dating is usually performed by measuring the loss of the parent radionuclide (^{14}C) in the dissolved inorganic carbon (DIC) of a given groundwater sample. Because chemical reactions and the evolution of carbonate systems may dilute the initial ^{14}C activity in the DIC, this age must be adjusted geochemically (Clark & Fritz, 1997; Kalin, 2000; Vogel, 1970). Carbon-13-mixing models (e.g., Fontes & Garnier, 1979; Ingerson & Pearson, 1964) are very useful in correcting ^{14}C ages. These adjustment models use measured ^{13}C , combined with ^{14}C activity and a series of other parameters (e.g., alkalinity, pH, and temperature).

The objectives of this study are four-fold: (a) to evaluate groundwater flow patterns in the Guadalajara area, (b) to estimate groundwater residence times, (c) to assess contamination trends and aquifer vulnerability to surface sources, and (d) to provide recommendations for groundwater protection and management. The combination of methods presented here may also be applied to other catchments in Mexico.

This study uses the classification scheme developed by Hernández-Antonio et al. (2015). Based on groundwater composition and M3 (Laaksoharju, Skårman, Gómez, & Gurban, 2009), which is a principal component analysis code, groundwater samples were classified into four groups: cold groundwater, hydrothermal groundwater, polluted groundwater, and mixed groundwater. Cold groundwater (group CG) refers to water characterized by low temperatures, salinity, and Cl and Na concentrations; this groundwater is predominantly of the Na-HCO_3 -type. Typically, CG originates as recharge in the La Primavera Caldera and is predominantly found in wells in the upper Atemajac Valley. Hydrothermal groundwater (group HG) is characterized by its high salinity, temperatures, and Cl, Na, and HCO_3 content; it also contains minor elements, such as Li, Mn, and F. This water is a mixed- HCO_3 -type found in wells from Toluquilla Valley and has undergone regional circulation through basaltic and andesitic rocks. Polluted groundwater (group PG) is characterized by elevated nitrate and sulfate concentrations and is usually derived from urban water cycling and agricultural return flow. Mixed groundwater (group MG) features properties between those of the cold, hydrothermal, and polluted types and is predominantly found in the lower Atemajac Valley.

2 | STUDY AREA

The Guadalajara Metropolitan Area (GMA) is located in the western portion of the Mexican Volcanic Belt, a Plio-Quaternary E–W-trending alkaline and subalkaline volcanic province (Campos-Enríquez,

Domínguez-Méndez, Lozada-Zumaeta, Morales-Rodríguez, & Andaverde-Arredondo, 2005), consisting of nearly 8,000 volcanic structures and several intrusive bodies (Demant, 1978). The Mexican Volcanic Belt (which is approximately 1,000 km long) crosses central Mexico from the Pacific Ocean to the Gulf of Mexico. The study area (1,368 km²) has a warm temperate climate with an average annual temperature of approximately 19.5 °C and an average annual rainfall of 989 mm in the north-central region and 904 mm in the south-central region (CONAGUA, 2015a, 2015b). The most important waterway in this area is the Santiago River, which flows through a canyon that is over 500 m deep to the east and north of the GMA (Figure 1). The Atemajac and Toluquilla Valleys comprising the GMA are bordered by hills, volcanic cones (El Cuatro, San Martín, and El Colli), plateaus (Tonalá), and volcanic calderas (La Primavera), among other features (Sánchez-Díaz, 2007). A more detailed description of the tectonic setting is given in Hernández-Antonio et al. (2015).

The Atemajac and Toluquilla Valleys feature a relatively thin cover of Quaternary lacustrine deposits overlying a thick section of Neogene volcanic rocks, including silicic domes, lava and cinder cones, lithic tuffs, basalts, ignimbrites and other pyroclastic rocks, andesitic lavas and volcanic breccias, and an Oligocene granite basement (Campos-Enríquez et al., 2005; Gutiérrez-Negrín, 1988; Urrutia-Fucugauchi et al., 2000).

Hydrogeologically, these valleys are underlain by two aquifers (Figure 2). The upper aquifer consists of alternating layers of pumice sand and ash flow tuff (the Tala Tuff) with interbedded lava flows. These units comprise a 450-m-thick unconfined aquifer with hydraulic conductivities ranging from 1.6×10^{-7} to 2.0×10^{-4} m/s (CONAGUA, 2015a, 2015b; Sánchez-Díaz, 2007). The groundwater recharge sources of this aquifer are rainwater and water ascending vertically from the lower aquifer (Gutiérrez-Negrín, 1991). Here, groundwater flows through faults and the Tala Tuff towards the central and northern regions of the study area. Pumping wells are drilled in the upper aquifer, reaching depths of 500 and 380 m in the Atemajac and Toluquilla Valleys, respectively. Figures 1 and 2 display a map and cross-sections of the aquifer. The water table is 150 m below ground level in the Atemajac Valley and 50 m below ground level in the Toluquilla Valley (SIAPA, 2004). In the Atemajac Valley, the direction of groundwater flow is mainly oriented from the southwest to the northeast, moving from topographically higher areas towards the Santiago River, with possible recharge originating from normal faults west of Guadalajara city (Figure 2, Section I). In contrast, groundwater flow in Toluquilla circulates from the northwest to the southeast (Figure 2, Section II; SIAPA, 2004; CONAGUA, 2009). Over the past several decades, depression cones resulting from excessive pumping have locally

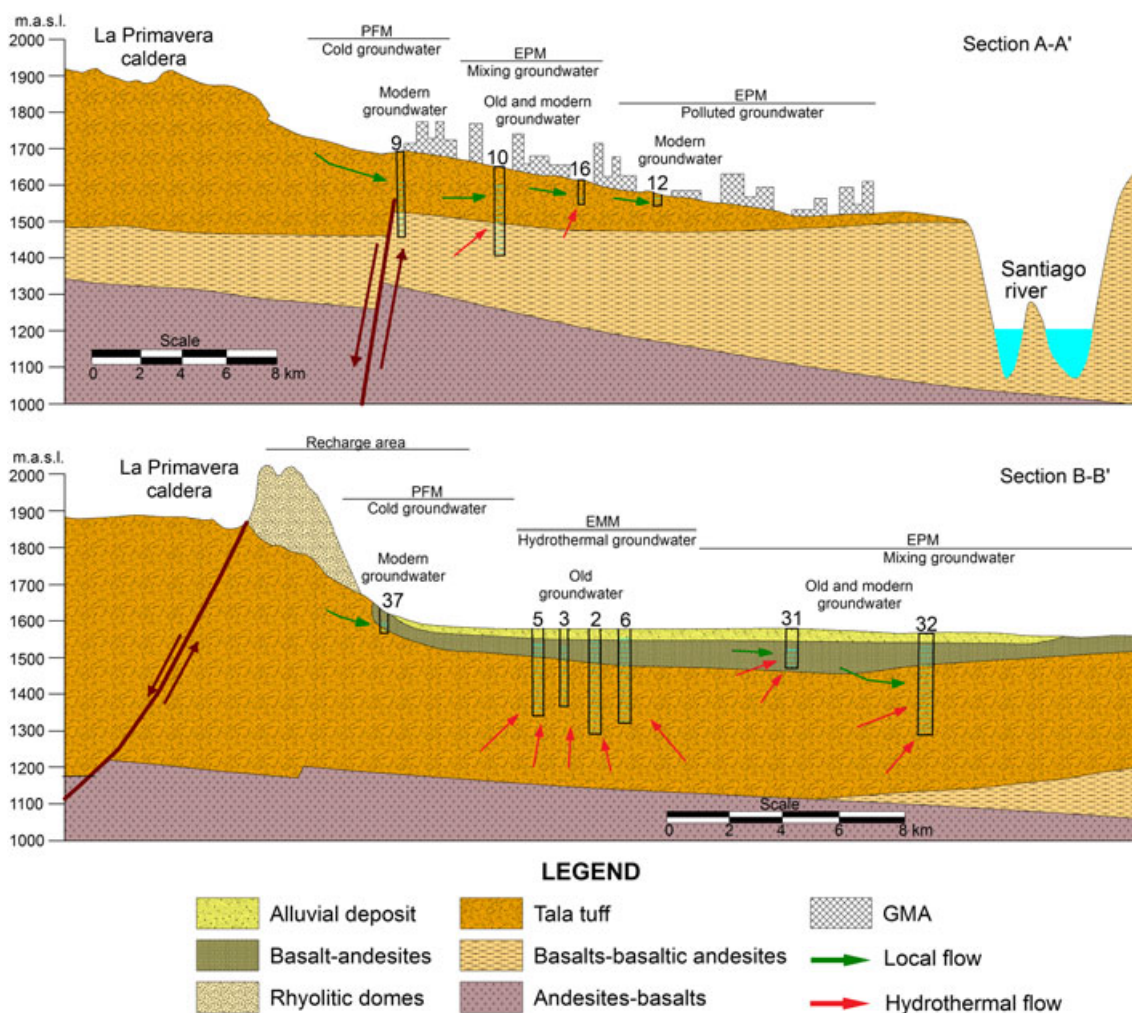


FIGURE 2 Hydrogeological sections of the Atemajac-Toluquilla aquifer system as indicated in Figure 1. Lumped parameter models are applied according to groups. PFM = piston flow model; EPM = exponential piston-flow model; EMM = exponential mixing model

modified these flow paths. Most discharge occurs through wells and from springs in the escarpment of the Santiago River Canyon (CONAGUA, 2015a, 2015b; SIAPA, 2004). Due to this heavy extraction from the aquifer system, water table levels are falling by an average of 2.2 m/year and 0.3 m/yr in the Atemajac and Toluquilla aquifers, respectively (SIAPA, 2004).

The lower aquifer consists of Pliocene-age andesites, rhyolites, and rare basalts with secondary permeability caused by fractures and hydraulic conductivities ranging from 10^{-8} to 10^{-4} m/s. Groundwater in this semiconfined to confined aquifer undergoes regional flow circulation in a southeast-northeast direction (Ramírez, del Razo, & Mata, 1982). This aquifer contains geothermal fluids and features a vertical upward flow, especially in the Toluquilla Valley (Venegas et al., 1991; SIAPA, 2004). Chloride mass balance calculations indicate that approximately 11% of water in the upper aquifer of the La Primavera caldera originates from the lower aquifer (Sánchez-Díaz, 2007).

3 | MATERIALS AND METHODS

3.1 | Field and laboratory methods

Twenty water samples collected from wells were analyzed for their major and minor ions, isotopic ratios (^2H , ^{18}O , ^{13}C), activities (^3H , ^{14}C) and gaseous concentrations (CFCs). Field parameters, such as temperature, pH, electrical conductivity (EC), and dissolved oxygen (DO), were measured using portable meters (Orion Star, Thermo Fisher Scientific, Waltham, MA, USA). Alkalinity was determined in the field using volumetric titration ($0.02\text{ N H}_2\text{SO}_4$) to achieve a pH of 4.3 in filtered water samples. At each sampling site, new and prerinced low-density polyethylene bottles were filled with filtered ($0.45\ \mu\text{m}$) sample water for analysis of anions, cations, stable water isotopes, and tritium. All groundwater samples were obtained by tapping wells during production. Borehole depth and water table depth varied from 24 to 300 m below ground level and from 25.0 to 94.6 m below ground level, respectively (Table 1). Wells were almost always completely screened.

Samples used for cation and silica measurements were acidified using ultrapure HCl to reach a pH of <2 , and all samples were stored in the laboratory at a constant temperature of $4\ ^\circ\text{C}$. Dissolved cations and anions were measured using inductively coupled plasma mass spectrometry and ion chromatography, respectively. Duplicates of selected samples were analyzed using inductively coupled plasma optical emission spectrometry and ion chromatography, following standard methods (APHA, 2012).

Samples analyzed for their $\delta^{18}\text{O}\text{-H}_2\text{O}$ and $\delta^2\text{H}\text{-H}_2\text{O}$ compositions were collected in 0.1-L glass bottles and measured using the $\text{H}_2\text{O}\text{-H}_2$ equilibration method (^2H), which has an analytical precision of $\pm 1.0\%$, and the $\text{H}_2\text{O}\text{-CO}_2$ equilibration method (^{18}O), which has an analytical precision of $\pm 0.15\%$ when obtained with an isotope ratio mass spectrometer (MM 903; VG Isogas Ltd, Middlewich, UK). These results are reported as δ -values with respect to the Vienna Standard Mean Ocean Water standard.

Sample collection and measurement of CFC-11 (CCl_3F), CFC-12 (CCl_2F_2), and CFC-113 ($\text{CCl}_2\text{FCClF}_2$) were performed using the methods described by Oster, Sonntag, and Münnich (1996). Samples

were collected in 500-mL glass flasks with ground necks that were stored in water-filled containers to prevent contamination. After undergoing preconcentration using a purge-and-trap technique, analyses were performed at Spurenstofflabor, Wachenheim, Germany, on a gas chromatograph with an electron-capture detector. These results are reported in pmol/L. The detection limit was close to 10^{-4} pmol/L, thus allowing the measurement of CFC concentrations as low as 0.01 pmol/L. For water samples, the measured 1σ reproducibility was better than $\pm 5\%$.

Tritium (^3H) was analyzed at the Environmental Isotope Laboratory, University of Arizona (Tucson, AZ, USA). The electrolytical enrichment method used was similar to that of Oestlund and Werner (1962). Counting was performed using a Quantulus 1220 liquid scintillation spectrophotometer (PerkinElmer, Waltham, MA, USA). Tritium concentrations are reported in tritium units (TU), in which 1 TU is equal to one tritium atom in 10^{18} hydrogen atoms. The detection limit was 0.3 TU, and the analytical precision of each measurement was typically better than $\pm 10\%$.

Carbon-13 (^{13}C) measurements were performed, using a Finnigan Delta S spectrometer (Thermo Fisher Scientific, Waltham, Massachusetts, USA), on carbon dioxide previously released by acidifying sample water (McCrea, 1950). These results are reported in $\delta^{13}\text{C}_{\text{DIC}}$ with respect to the Vienna Pee Dee Belemnite (VPDB) standard and feature an analytical precision of 0.15% ($1\text{-}\sigma$). Radiocarbon activity was measured by accelerator mass spectrometry at the NSF-Arizona Accelerator Facility for Radioisotope Analysis (Tucson, AZ, USA) and is reported as percent modern carbon (pMC). The analytical precision ($1\text{-}\sigma$) ranged from 0.1 pMC (for pMC values near zero) to 0.5 pMC (for pMC values near 100 pMC).

3.2 | Interpretation methods

Chlorofluorocarbons are environmental tracers that can be used to date young groundwater (Mahlknecht et al., 2006b; Newman et al., 2010; Stewart, Morgenstern, McDonnell, & Pfister, 2012). The atmospheric concentration of CFCs is relatively uniform in the Northern Hemisphere, which facilitates the calculation of initial mixing ratios in groundwater. However, local sources from cities and industries, sorption, or even the sampling process may affect the levels of CFCs measured within a sample (Plummer et al., 2001). Additionally, microbial degradation may occur under reducing conditions (Cook & Solomon, 1995; Plummer et al., 1998). In the aquifer system studied here, it is unlikely that microbial degradation of CFCs has taken place due to its generally oxic conditions, in which the DO content ranges between 3.3 and 7.9 mg/L (Table 1). However, contamination from local sources, such as industries and landfills, as well as return flow from irrigated land, makes it challenging to perform accurate age dating on these samples. In several cases, various CFCs do not yield concordant ages. Tritium concentrations are frequently near the limit of detection, which also prevents correct age dating. Thus, in this study, CFCs and tritium were only used as qualitative age tracers.

Radiocarbon was used to evaluate older ($>1\text{ ka}$) groundwater in the Atemajac-Toluquilla aquifer system. Unadjusted ^{14}C ages were calculated from measured ^{14}C activities of DIC using the Libby half-life (5,568 years) and assuming an initial ^{14}C activity (a_0) of 100% modern carbon (pMC). In the age-adjustment process, samples were divided

TABLE 1 Well information, field parameters, ion concentrations, carbon dioxide partial pressure, saturation indices, and oxygen-18 ratios. Data are given in mg/L, except where otherwise indicated

Well ID group	Well name	Well depth (m)	Depth to WT (m)	pH (S.U.)	T (°C)	EC ($\mu\text{S cm}^{-1}$)	DO	Na	K	Ca	Mg	Cl	HCO ₃	SO ₄	NO ₃ -N	SiO ₂	F	Li	Mn	Log P _{CO₂} (-)	Log SI CaCO ₃ (-)	SI dol (-)	$\delta^{18}\text{O}$ (‰ VSMOW)	$\delta^2\text{H}$ (‰ VSMOW)	
9	CG	Tapatíos 1	258	94.6	6.2	25.0	310	6.6	57.3	7.2	2.3	3.7	122.0	12.3	4.7	52.6	0.97	0.09	<0.01	-1.1	-2.3	-4.4	-9.8	-71.1	
17	CG	Bajo La Arena B	80	61.7	8.7	24.6	219	4.3	20.8	1.8	0.5	0.7	53.7	2.2	2.4	48.3	1.40	<0.05	<0.01	-3.7	0.2	-4.7	-9.9	-72.2	
29	CG	Testistan 56	270	92.2	6.9	33.7	298	7.7	16.7	1.7	2.1	7.6	30.5	21.0	6.8	19.1	0.22	<0.05	<0.01	-2.0	-1.8	-5.8	-9.3	-66.5	
30	CG	Testistan 70	250	65.3	7.1	26.0	108	4.8	20.0	8.8	1.9	2.9	60.8	12.3	5.7	47.5	0.39	<0.05	<0.01	-2.3	-2.3	-4.1	-9.4	-67.8	
34	CG	El Lindero	55	61.9	6.7	26.6	139	6.6	22.2	7.4	5.5	1.2	97.6	6.1	2.0	40.8	0.18	<0.05	<0.01	-2.0	-2.5	0.6	-9.6	-68.9	
35	CG	Vivero Los Amigos	24	41.3	6.6	27.3	235	7.7	19.9	16.6	10.1	4.1	2.7	53.7	40.1	25.4	30.9	0.03	<0.05	<0.01	-1.5	-1.9	-1.7	-9.4	-64.5
37	CG	Viveros del Sur	54	75.2	6.3	27.7	160	5.6	14.1	0.6	1.9	0.3	2.1	29.3	2.1	1.2	20.3	4.90	<0.05	0.02	-1.4	-2.5	-3.2	-10.3	-71.6
12	PG	Agua Azul	40	25.0	7.1	29.1	354	3.3	44.1	8.9	23.0	7.4	50.3	24.4	11.8	41.4	0.20	<0.05	<0.01	-1.8	-0.8	-4.0	-5.7	-47.5	
10	MG	Topacio	235	57.9	6.7	21.8	569	6.3	63.8	21.0	14.3	6.3	5.2	242.2	8.9	0.4	38.4	0.84	<0.05	<0.01	-1.8	-1.4	-1.9	-8.9	-71.5
16	MG	Fray Pedro	70	56.5	7.3	30.0	334	4.3	21.0	6.5	4.6	2.2	5.6	68.3	8.5	1.4	20.1	0.34	<0.05	<0.01	-2.1	-0.7	-3.6	-8.7	-62.4
21	MG	La Loma de S. Juan	60	59.4	7.5	25.3	569	4.4	38.3	8.6	16.7	12.9	7.2	172.2	6.1	1.0	44.3	0.46	<0.05	<0.01	-2.5	-0.8	-1.2	-9.5	-67.8
31	MG	Unid. Dep. Tonalá	118	76.7	6.7	29.8	351	3.5	40.3	12.7	13.3	7.6	3.4	181.8	1.7	1.1	35.2	0.26	<0.05	<0.01	-1.7	-2.0	-1.3	-9.0	-65.6
32	MG	San Ismael	285	41.6	6.7	23.9	451	4.4	20.2	7.5	15.8	7.8	0.3	132.2	0.2	0.1	33.6	0.06	<0.05	<0.01	-1.8	-1.4	-0.9	-8.8	-64.8
36	MG	El Taray	200	91.8	6.4	24.7	242	4.4	11.5	7.8	9.3	4.7	0.5	102.5	0.3	0.1	36.0	0.26	<0.05	<0.01	-1.2	-2.1	-0.5	-9.3	-67.1
2	HG	Toluquilla 6	300	36.9	7.0	25.0	1619	5.8	152	58.0	28.9	103	70.1	1069	6.5	<0.04	38.5	0.33	0.3	0.3	-1.0	-0.2	-0.3	-9.3	-68.4
3	HG	Toluquilla 17	200	54.6	7.0	25.0	2310	5.3	114	36.0	58.7	92.9	82.4	1031	5.0	0.1	35.1	0.65	0.3	0.5	-1.0	0.1	0.0	-8.8	-66.5
4	HG	Toluquilla 22	300	38.3	7.0	31.8	1792	5.1	147	40.9	89.7	113	85.4	1415	6.6	<0.04	53.6	0.99	0.4	0.2	-0.8	0.5	0.4	-9.1	-67.4
5	HG	Toluquilla 7	230	42.4	7.0	36.4	1900	5.5	174	48.4	80.7	104	229	697.6	22.4	<0.04	61.6	3.50	0.5	0.8	-1.1	0.2	0.2	-8.9	-66.5
6	HG	Las Pintas	250	25.1	7.2	33.6	718	6.2	102	33.9	31.2	16.0	14.5	435.2	5.9	0.0	40.0	0.26	<0.05	0.0	-1.5	-0.1	-0.2	-8.8	-64.7
22	HG	Rancho Alegre	150	33.8	7.7	27.5	214	4.5	92.6	28.5	37.3	47.8	41.5	467.9	19.6	0.8	46.6	0.94	0.16	0.13	-2.9	-1.2	-0.7	-9.3	-66.3

Note. T = temperature; EC = electrical conductivity; DO = dissolved oxygen; WT = water table. Water samples were classified into four groups according to Hernández-Antonio et al. (2015), based on multivariate analysis: CG = cold groundwater; PG = polluted groundwater; MG = mixed groundwater; HG = hydrothermal groundwater.

into two groups and treated differently. Age adjustments for samples in the recharge area (group CG) were made using the formula-based F&G adjustment model (Fontes & Garnier, 1979). This model considers a two-stage evolution of recharge waters, accounting for the dissolution and isotopic exchange of carbonate minerals with CO₂ in the unsaturated zone, as well as isotopic exchange with carbonate rocks in the saturated zone (Clark & Fritz, 1997; Plummer & Glynn, 2013; Plummer, Prestemon, & Parkhurst, 1991).

Age adjustments for nonrecharge samples (groups MG and HG) were performed using NetPathXL (Parkhurst & Charlton, 2008), which is a revised version of NETPATH (Plummer, Prestemon, & Parkhurst, 1994) that runs under Windows operating systems. NETPATH is a computer program that uses inverse geochemical modeling techniques to calculate net geochemical reactions that can account for changes in the chemical and isotopic compositions of water between initial and final evolutionary waters in hydrologic systems. It can also estimate radiocarbon ages of dissolved carbon in groundwater. The inverse geochemical approach was applied along approximate flow sections, and these results represent chemical transfer rates between initial and final wells. As demonstrated in a previous study (Hernández-Antonio et al., 2015), normal faults can facilitate the vertical upward flow of hydrothermal fluids from lower regions to upper units; this must be taken into consideration during the geochemical modeling process. Therefore, we attempted to model the evolution of each final water sample (represented by nonrecharge samples from groups MG and HG) as the result of mixing recharge water (represented by samples from group CG) with hydrothermal fluids. The composition of the hydrothermal fluid was defined as that of deep well PP-1 ($T = 255\text{ }^{\circ}\text{C}$, $\text{Cl} = 851\text{ mg/L}$, $\text{B} = 120\text{ mg/L}$, $\text{Li} = 9.9\text{ mg/L}$, and $\text{Na} = \text{mg/L}$), which is located in the La Primavera geothermal field (Maciel-Flores & Rosas-Elguera, 1992). Reaction equations were derived from the NETPATH database. The constraints used in these models were Ca^{2+} , Mg^{2+} , HCO_3^- , SO_4^{2-} , Cl^- , SiO_2 , and carbon-13; the phases used were CO₂ (gas), calcite, gypsum, albite, potassium feldspar, biotite, halite, amorphous silica, Ca/Na ion exchange, and kaolinite. These phases are believed to be reactive, based on lithological and mineralogical data (Mahood, 1980, 1981; Sánchez-Díaz, 2007) and geochemical stability calculations (Morán-Ramírez, Ledesma-Ruiz, Mählknecht, & Ramos-Leal, 2016). The initial ¹⁴C value (A_0) is adjusted for the modeled geochemical reactions along a flow path between the initial and final water samples. The program constructs a series of geochemical adjustment models to estimate the ¹⁴C content of TDC in water from well B without radioactive decay (A_{nd}). The travel time between A and B can be calculated from the decay equation as follows:

$$\Delta t = \frac{5730}{\ln 2} \ln \frac{A_{nd}}{A_{obs}}$$

where A_{obs} represents the measured ¹⁴C values of groundwater samples. A series of models (original data, mass balance, Vogel, Tamers, Mook, and Fontes & Garnier) were used to compute A_{nd} , and a range of obtained ages are reported to account for uncertainty (Plummer et al., 1994).

Several assumptions were made for both the recharge and nonrecharge waters. The ¹⁴C activity and $\delta^{13}\text{C}$ value of dissolved carbonate minerals were set as 0 pMC and 0‰ VPDB, respectively. The

¹⁴C activity of soil CO₂ in all samples is approximately 100 pMC (Kalin, 2000), with the exception of sample no. 35, which is clearly a modern water sample and therefore has a higher initial activity of 105 pMC, as has been reported in previous studies (e.g., Horst, Mählknecht, López-Zavala, & Mayer, 2011). The $\delta^{13}\text{C}$ value of soil CO₂ was set as -18‰ VPDB to account for the assortment of C3 and C4 plants in the recharge area. Isotopic fractionation factors were calculated using the methods of Vogel, Grootes, and Mook (1970); Mook, Bommerson, and Staverman (1974); and Deines, Langmuir, and Harmon (1974).

4 | RESULTS

4.1 | Groundwater chemistry and stable isotopes

Analytical results for physicochemical parameters, ionic concentrations, and isotopic ratios are listed in Table 1. Groundwater samples record relatively neutral pH values, ranging from 6.2 to 8.7 (with an average value of 7.0), temperatures ranging from 21.8 to 36.4 °C (average 27.4 °C), and highly variable EC values ranging from 108 to 2310 μS/cm (Table 1). DO concentrations vary between 3.3 and 7.7 mg/L, suggesting variable oxidation conditions. In general, the dominant cations are $\text{Na} > \text{Ca} > \text{Mg} > \text{K}$, and the dominant anions are $\text{HCO}_3^- > \text{Cl}^- > \text{SO}_4^{2-} > \text{NO}_3^- > \text{F}^-$. Chloride, nitrate, sulfate, and fluoride are of particular interest because they were considered to be contaminants in several previous studies (IMTA (Instituto Mexicano de Tecnología del Agua), 1992; SIAPA, 2004; Sánchez-Díaz, 2007). The concentrations of these elements measured in this study range from 0.3 to 229 mg/L (chloride), 0 to 25.4 mg/L (nitrate), 0.2 to 95.2 mg/L (sulfate), and 0 to 4.9 mg/L (fluoride).

Stable water isotopes may provide information about the origin of groundwater and its subsequent evaporation processes. Oxygen-18 and ²H concentrations vary from -10.3 to -5.7‰ and from -72.2 to -47.5‰, respectively (Table 1). Figure 3a compares these groundwater values with those of with global (Rozanski, Araguás-Araguás, & Gonfiantini, 1993) and regional (Wassenaar, Van Wilgenburg, Larson, & Hobson, 2009) meteoric water lines (GMWL and RMWL, respectively). This comparison suggests that the groundwater sampled in this study is of meteoric origin that has undergone varying degrees of evaporation and mixing with hydrothermal fluids (Figure 3a,b). Previous investigations (IMTA (Instituto Mexicano de Tecnología del Agua), 1992) observed a similar trend. Hydrothermal groundwater records a narrow range of ¹⁸O (-9.3 to -8.8‰) and ²H (-68.4 to -64.7‰) values (Table 2). In general, it tends to fall slightly below and parallel to the RMWL, likely representing the incorporation of precipitation of a different origin, such as rainstorms originating from outside the basin limits (e.g., Mählknecht, Schneider, Merkel, de Leon, & Bernasconi, 2004). These samples also record isotopic depletion, indicating that recharge by meteoric water is low; this is further supported by the presence of a deuterium excess ranging from 4 to 8‰, with an average value of 5.5‰ (Hernández-Antonio et al., 2015).

4.2 | Groundwater age

A direct indicator of groundwater flow and the migration of contaminants is that of groundwater age. Age tracer results are shown in

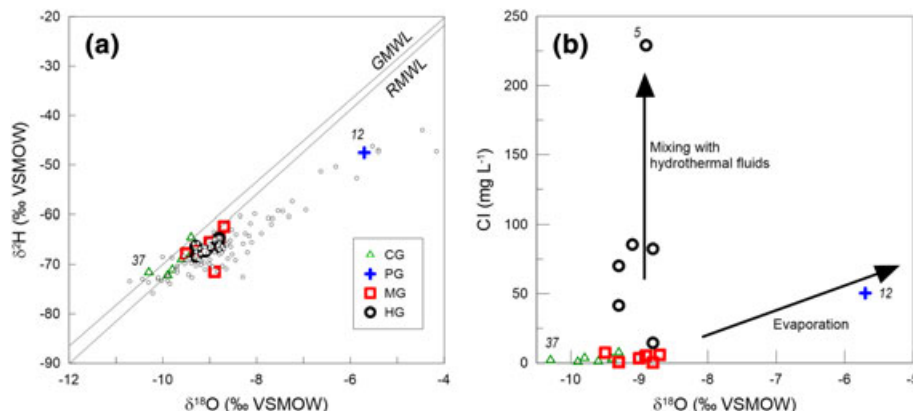


FIGURE 3 (a) Deuterium and oxygen-18 compositions in groundwater from the Atemajac–Toluquilla aquifer system, based on well groups and findings from previous studies (IMTA (Instituto Mexicano de Tecnología del Agua), 1992; SIAPA, 2004); (b) oxygen-18 vs. chloride concentrations. GMWL = global meteoric water line (Rozanski et al., 1993); RMWL = regional meteoric water line (Wassenaar et al., 2009); VSMOW = Vienna Standard Mean Ocean Water

Table 2. Tritium values in groundwater samples range from 0.3 to 3.0 TU. The activity of ^3H in rainwater in Central Mexico has been decreasing since the 1960s and finally dropped below 3 TU in 2007 (Horst et al., 2008); it is estimated that the current tritium level has since stabilized between 2 and 3 TU (Figure 4). A graph of ^3H and ^{14}C values reveals two different trends (Figure 5a). First, samples with elevated ^3H values (>1.5 TU) and relatively high ^{14}C values (>80 pMC) represent young waters or recent recharge that have undergone little mixing with other waters; these are located primarily in the La Primavera volcanic system. These waters record increasing $\delta^{13}\text{C}$ with increasing ^{14}C (except for sample no. 9; Figure 5b), low EC, Cl, DIC, and temperatures (Figure 5c, d), and high nitrate concentrations ($\text{NO}_3\text{-N} > 1$ mg/L; Figure 5e). The high $^{14}\text{C}/\delta^{13}\text{C}$ endmember has a $\delta^{13}\text{C}$ value of approximately -8‰ . The second trend observed in Figure 5a is vertical, in which all samples record low concentrations of tritium (largely <1 TU) and variable ^{14}C values (1 to 60 pMC). In this trend, $\delta^{13}\text{C}$ increases from -14 to -2‰ with decreasing ^{14}C values. Samples in this set mainly consist of prebomb water samples. The presence of a small but detectable amount of tritium in many samples with very low ^{14}C values (<10 pMC) indicates that some mixing with postbomb recharge may have occurred, even in samples that appear to represent the oldest prebomb groundwater samples. However, as mentioned above, low tritium values close to the detection limit (<0.7 TU; No. 5, 16, and 22) may not be true values, as the detectable tritium values in hydrothermal and mixed groundwater samples could easily have come from bore leakage. Low- ^{14}C waters are found mostly in Toluquilla and record elevated EC, Cl, and DIC values and low nitrate concentrations ($\text{NO}_3\text{-N} < 0.1$ mg/L, Figure 4e). They have enriched ^{18}O values (-8.7 to -9.3‰) relative to cold water (-9.3 to -10.4‰), which are lower in ^{18}O ; isotopic values of mixed waters lie between these two endmembers, as is expected (Table 1, Figure 5f).

All samples record detectable levels of CFCs (Table 2), which indicates that all sampled groundwater contains at least a small fraction of water recharged after 1940. Closer analysis of these results reveals additional information. For example, sample 12 (Agua Azul), which was collected from the Guadalajara urban area, is an outlier, indicating that it was affected by local pollution and is therefore not viable for

age dating. Figure 6a demonstrates that samples 22 (Rancho Alegre) and 35 (Vivero Los Amigos) do not fall on the CFC-11/CFC-12 model curves, thus indicating that they have been contaminated by CFC-11 and CFC-12. Sample 35 was collected from the recharge area, and sample 22 was collected from a recreational area far from any urban area or obvious CFC source. Therefore, their increased CFC concentrations may be attributed to contamination with CFC compounds during sampling or from a nearby landfill. The anomalous CFC-11/CFC-12 ratios plotting off the model line could also be due to the degradation of CFC-11 or CFC-12 (Plummer, Busenberg, & Cook, 2006). Figure 6b indicates that most CFC-12 and CFC-113 data plot along the exponential mixing and dispersion line, thus demonstrating the viability of these two LPM models. As mentioned above, points lying off of this curve may indicate that contamination or degradation of CFC-12 and/or CFC-113 has occurred (Plummer et al., 2006). Samples 29 (Tesistan 56) and 30 (Tesistan 70) were obtained from the recharge area and may thus reflect contamination occurring during the sampling process. The relatively high proportion of contaminated samples can be explained by the fact that several samples were collected from sites in urbanized and industrialized areas, where potential CFC sources are ubiquitous.

Analysis of the spatial distribution of CFCs from noncontaminated sites in the study area indicates that CFC concentrations are generally higher in the Atemajac area than they are in Toluquilla (Figure 7a). This can be attributed to relatively shorter residence times in the fractured and fissured media of Atemajac. Inside the Toluquilla area, regions of higher concentrations coincide with elevated areas along the western border. Springs and wells tapping lower aquifer units in the southern and southeastern regions of the area have generally low CFC-12 concentrations compared to those observed in younger rocks in the northwestern and western regions. A similar trend is observed for radiocarbon concentrations (Figure 7b).

Radiocarbon age dating results are shown in Table 2. Unadjusted ^{14}C ages range from zero age to 39 ka. Adjusted ^{14}C ages for samples from recharge zones (group CG) are generally modern. More geochemically evolved samples (i.e., nonrecharge samples) yield ages ranging from modern to 14 ka in mixed groundwater samples and from 13 to 27 ka in hydrothermal water samples.

TABLE 2 Carbon isotopic data, tritium content, and CFC values for the Atemajac-Toluquilla aquifer system with corresponding residence time estimates and best fit models

ID	Well group	Well name	Description	³ H (TU)	Concentration				δ ¹³ C (‰)	Unadjusted ¹⁴ C age (ka)	Initial well	Hydro-thermal fluid contribution (%)	a ¹⁴ C (no decay, pMC)	Adjusted ¹⁴ C age (ka)
					CFC-11 (pmol/L)	CFC-12 (pmol/L)	CFC-113 (pmol/L)	a ¹⁴ C (pMC)						
9	CG	Tapatíos 1	Low temperature, salinity, and Cl and Na concentrations.	1.2	3.30	0.46	0.07	79.7	-1.0	20.9	-	-	modern	
17	CG	Bajo La Arena B	Predominantly of Na-HCO ₃ -type. Originates as recharge at "La Primavera" caldera and is found predominantly in wells in the upper Atemajac Valley. Cold, recent groundwater with little mixing.	0.9	1.10	0.70	0.11	68.0	-12.8	3.2	-	-	1.5	
29	CG	Tesistan 56		1.7	51.00	1.70	0.23	91.0	-8.9	0.8	-	-	modern	
30	CG	Tesistan 70		1.7	2.10	1.20	0.11	83.2	-10.9	1.5	-	-	modern	
34	CG	El Lindero		2.0	30.00	1.10	2.20	90.0	-8.7	0.9	-	-	modern	
35	CG	Vivero Los Amigos		2.9	2.80	1.60	0.26	103.5	-8.6	modern	-	-	modern	
37	CG	Viveros del Sur		0.5	1.60	1.00	0.15	72.2	-10.1	2.7	-	-	modern	
12	PG	Agua Azul	Elevated nitrate and sulfate concentrations. Derived from urban water cycling and agricultural return flow. Cold groundwater with mixing.	2.4	>600	>600	>800	98.2	-9.0	modern	-	-	-	modern
10	MG	Topacio	Properties between those of the cold and hydrothermal types.	0.9	1.60	8.70	0.08	21.7	-5.7	12.6	9	0.1	84.7-116.8	11.3-13.9
16	MG	Fray Pedro		0.3	8.00	1.30	0.30	27.6	-6.1	10.6	17	0.4	37.7-55.5	0.1-5.8
21	MG	La Loma de San Juan	Predominantly found in the lower Atemajac Valley. Mixing of old and recent groundwater.	0.8	0.80	0.54	0.10	35.6	-9.1	8.6	37	0.5	54.9-71.6	3.6-5.8
31	MG	Unidad Deportiva		0.7	0.30	0.18	0.04	34.9	-9.2	8.7	37	0.1	54.5-60.2	3.7-5.4
32	MG	Tonala		0.7	0.40	0.33	0.05	51.2	-12.9	5.5	37	0.4	73.6-77.4	3.0-3.4
36	MG	San Ismael		0.7	0.80	0.51	0.08	61.0	-13.8	4.1	37	0.1	75.2-78.5	1.7-2.1
2	HG	Toluquilla 6	High salinity, temperature, Cl, Na, and HCO ₃ , and the presence of minor elements such as Li, Mn, and F. Mixed-HCO ₃ type. Found in wells from Toluquilla Valley. Represents regional, confined circulation through basaltic and andesitic rocks.	0.7	0.67	0.38	0.05	3.7	-5.7	27.4	37	6.0	32.3-35.8	17.9-18.8
3	HG	Toluquilla 17		0.7	0.52	0.25	0.03	0.9	-2.2	38.9	37	6.5	12.9-16.8	22.0-24.2
4	HG	Toluquilla 22		1.2	1.10	0.54	0.07	1.6	-3.1	34.5	37	6.0	17.7-20.7	19.9-21.1
5	HG	Toluquilla 7		0.4	0.90	0.45	0.07	0.9	-2.6	39.2	37	21.5	15.1-23.2	23.3-26.8
6	HG	Las Pintas		0.9	0.70	0.46	0.07	7.6	-6.6	21.3	37	1.2	38.4-45.2	13.4-14.7
22	HG	Rancho Alegre		0.5	1.70	0.39	0.07	6.6	-4.7	22.5	37	3.7	27.7-35.2	11.8-13.8

Note. CG = cold groundwater; PG = polluted groundwater; MG = mixed groundwater; HG = hydrothermal groundwater; -, not applicable.

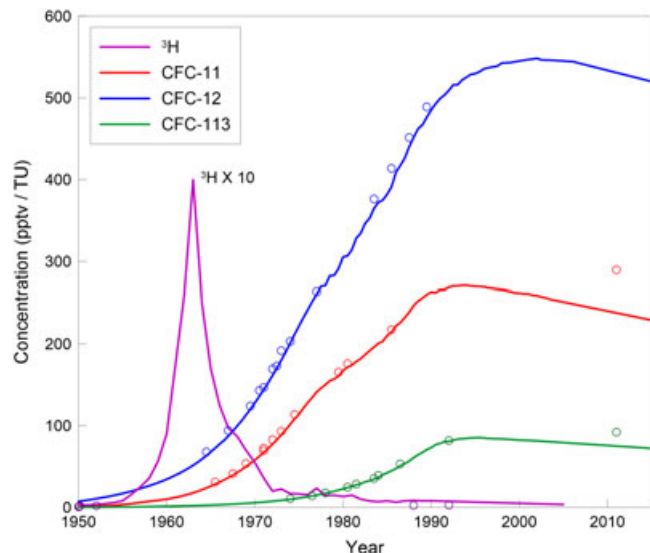


FIGURE 4 Atmospheric concentrations of transient tracers measured as a function of time. Tritium input function is estimated using the IAEA-GNIP network data from the two closest stations, Veracruz and Chihuahua (Horst, Mahlknecht, & Merkel, 2007). Chlorofluorocarbons (CFCs) were measured at Niwot Ridge, Colorado, USA (USGS, 2015)

5 | DISCUSSION

5.1 | Evaluation of groundwater flow patterns

Hydrogeological, chemical, and isotopic data indicate that local groundwater recharge is primarily caused by the infiltration of rainfall over the La Primavera caldera in the central-western region of the study area. Groundwater flows to the northeast (Atemajac Valley), east (Guadalajara), and southeast (Toluquilla Valley) through the upper

alluvial sediments towards the valley floor and the Santiago River. This groundwater is of the Na- HCO_3 water type, which is characterized by low temperatures, salinities, and Cl and Na contents, as well as elevated NO_3 concentrations and relatively high tritium (0.5–2.9 TU), CFC-12 (generally >1.0 pmol/L), CFC-13 (0.8–2.2 pmol/L), and radiocarbon (68–103.5 pMC) activities (Table 2). These data indicate that little mixing of flow paths has occurred and that recent recharge originated from pristine soils and return flow from agricultural plots.

In general, the temperature and salinity of the groundwater increase along the flow path through the upper aquifer (alluvial sediments and Tala Tuff) due to the admixture of regional groundwater from the lower aquifer unit (basaltic-andesitic rock formations) and hydrothermal fluids produced by the magma chamber below La Primavera Caldera. Geochemical modeling indicates that the contribution of hydrothermal waters approaches 0.5% in the northern-central region (Atemajac Valley) and 20% in the southern region (Toluquilla Valley; Table 2). Groundwater in deep wells from the Toluquilla area are Mg- HCO_3 and mixed HCO_3 waters, characterized by elevated temperatures, salinity, and Cl, Na, and HCO_3 contents, as well as low contents of tritium (<1.7 TU), CFC-12 (0.3–0.5 pmol/L), CFC-13 (0.03–0.07 pmol/L), and radiocarbon (0.9–6.6 pMC). The isotopic composition of this groundwater thus confirms that the waters from shallow and deep rock materials are interconnected.

A second, more local trend is observed in groundwater that circulates through the upper aquifer (i.e., the Tala Tuff Formation) in the direction of urban Guadalajara. These waters are affected by anthropogenic pollution, resulting in the generation of a Na- SO_4 to mixed- HCO_3 water type with relatively high contents of SO_4 , NO_3 , Na, Cl, and tritium (>2 TU). In general, these sites record CFC contamination that can potentially be attributed to landfills or industrial processes.

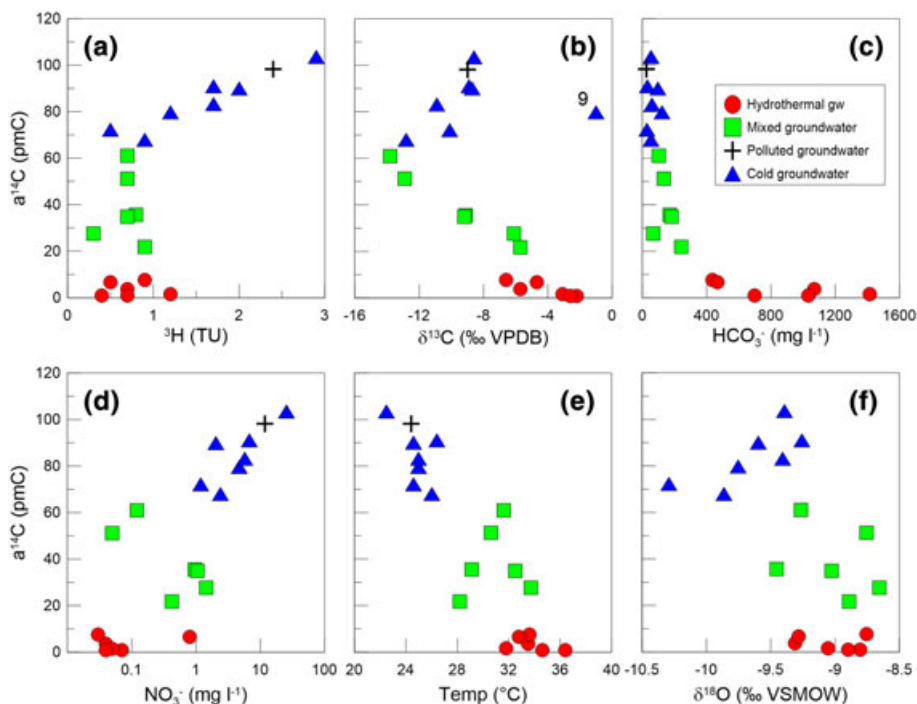


FIGURE 5 Radiocarbon activity in the Atemajac–Toluquilla aquifer system vs. (a) tritium, (b) carbon-13, (c) alkalinity, (d) nitrate content, (e) temperature, and (f) oxygen-18

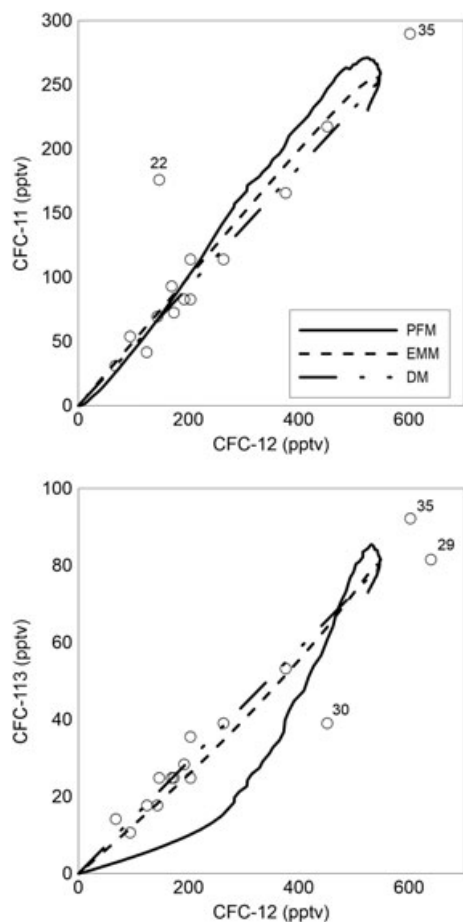


FIGURE 6 Mixing ratios of chlorofluorocarbons (CFCs) for collected groundwater and selected models: (a) CFC-11 vs. CFC-12 mixing ratios; (b) CFC-113 vs. CFC-12 mixing ratios. PFM = piston flow model; EMM = exponential mixing model; DM = dispersion model. Sample 12 falls outside the plot area

5.2 | Assessment of groundwater ages

To a first order, the presence of detectable CFCs and tritium in groundwater is evidence that post-1950 recharge has occurred in the study area. However, the presence of CFCs and tritium in more evolved groundwater samples indicates that water leakage has occurred between the upper and lower aquifer units in the well. This is a very common aspect of Mexican public wells, which are almost always completely screened and thus capture different aquifer units. These wells may also be affected by return flow in irrigated areas, especially in Toluquilla (Horst et al., 2008; Mahlknecht et al., 2006a; Mahlknecht et al., 2008).

The cold groundwater of the upper aquifer likely underwent mixing with lower-aquifer water to a detectable extent, so that its CFC concentrations were not attenuated. The geochemical data presented in Figure 5 are consistent with mixing between upper and lower aquifer waters (i.e., mixed and hydrothermal group waters); waters in the upper aquifer's "cold groundwater" category are consistent with having undergone mixing with different types of dissolved rock carbon.

The interpretation of CFC gas tracers depends on the age of the atmosphere preserved in the infiltrating water as it reaches the water table, which ranges in its depth from 25.0 to 95.6 m below ground level

(Table 1). Because of diffusion processes, travel time delays or lag times of up to 30 years can occur. This indicates that mean residence time values must be reduced by these lag time values in order to obtain correct age estimates. Cook and Solomon (1995) and later Engesgaard et al. (2004) each developed an analytical correction model assuming exponential or linear increases, respectively, of CFCs in the unsaturated soil zone; these models can be applied to correct for this lag time. However, these correction models do not take into account the continuously declining water table (which has receded by some tens of meters over the past 50 years), barometric pumping (Nilson, Peterson, Lie, Burkhard, & Hearst, 1991), and considerable groundwater fluctuations (Li & Jiao, 2005). Therefore, residence times computed from CFCs are erratic.

Radiocarbon activities are generally less influenced by water table fluctuations, pumping, and sampling because the atmospheric partial pressure of CO_2 is lower than that of soil CO_2 , and degassing only produces minor fractionation (Clark & Fritz, 1997). This explains why CFC- ^{14}C tracer-tracer plots often do not match. Additionally, the CFC age values of hydrothermal water are older than the maximum age that can be measured by CFC age dating (50 years), which makes this tracer a less reliable age indicator. These observations demonstrate that measured CFC values can better serve as an indicator of potential surface contamination than as an age dating tool.

The combination of P_{CO_2} , DIC, and $\delta^{13}\text{C}_{\text{DIC}}$ data can reflect recharge conditions (Li et al., 2015). The calculated P_{CO_2} of samples 12 and 35, which have shallow well depths of 40 and 25 m, respectively, is similar to that of soil (approximately $10^{-1.8}$ units; Clark & Fritz, 1997), which represents calcite dissolution occurring under open conditions (Table 1). In contrast, the $\delta^{13}\text{C}$ values of these samples (-9.0 and -8.6 ‰, respectively) indicate that the $\delta^{13}\text{C}_{\text{soilCO}_2}$ is approximately -18 ‰ under the given pH conditions (7.1 and 6.6 pH units). This value represents a combination of C_3 and C_4 organic material, which is consistent with the mixed vegetation appearing in recharge areas, namely, grassland and shrubland with *Quercus* and *Pinus* as their major taxa, according to Zárate-del-Valle, Ramírez-Sánchez, Fernex, Simoneit, and Israde-Alcántara (2011).

5.3 | Assessment of contaminant evolution and aquifer vulnerability to surface sources

Wells and springs with different groundwater travel times (i.e., different geochemical ages) can be used to evaluate chemical differences in groundwater. In this study, groundwater ages are used to investigate possible chemical interactions and how they affect the geochemical evolution of the Atemajac-Toluquilla aquifer system. Analysis of ^{14}C data makes it possible to view differences between groups and observe changes along a flow path. We are thus able to determine relationships between groundwater ages and water quality parameters (Figure 8). For example, concentrations of chloride, Na, Li, and Mn are greater in hydrothermal waters than they are in cold and mixed waters, and their concentrations increase with increasing ^{14}C age.

In contrast, NO_3 contents are relatively high in some local cold waters but are insignificant in hydrothermal and mixed waters. This is important because all sites with high NO_3 contents are located in and near recharge zones in the western region of the study area (i.e.,

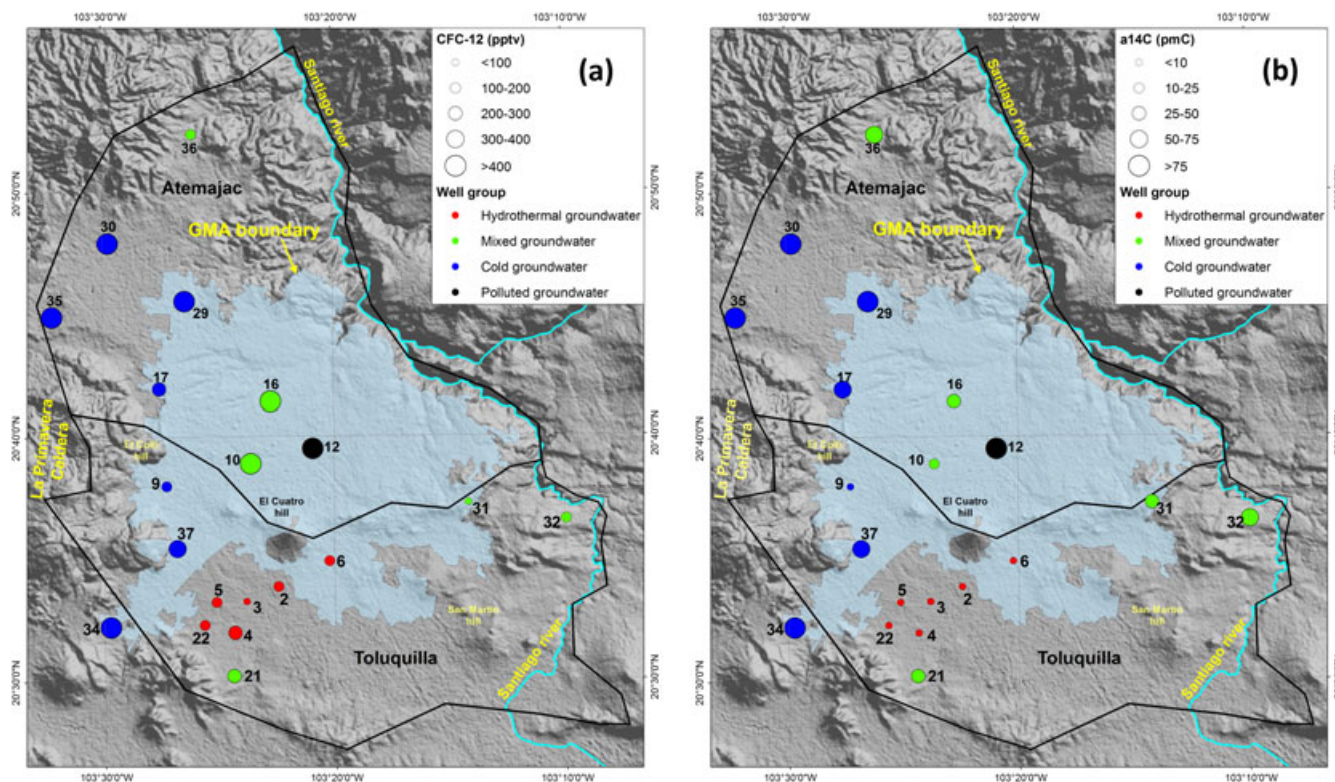


FIGURE 7 Spatial distribution of age tracers in groundwater of the Atemajac–Toluquilla aquifer system: (a) CFC-12 mixing ratios, (b) ^{14}C activities

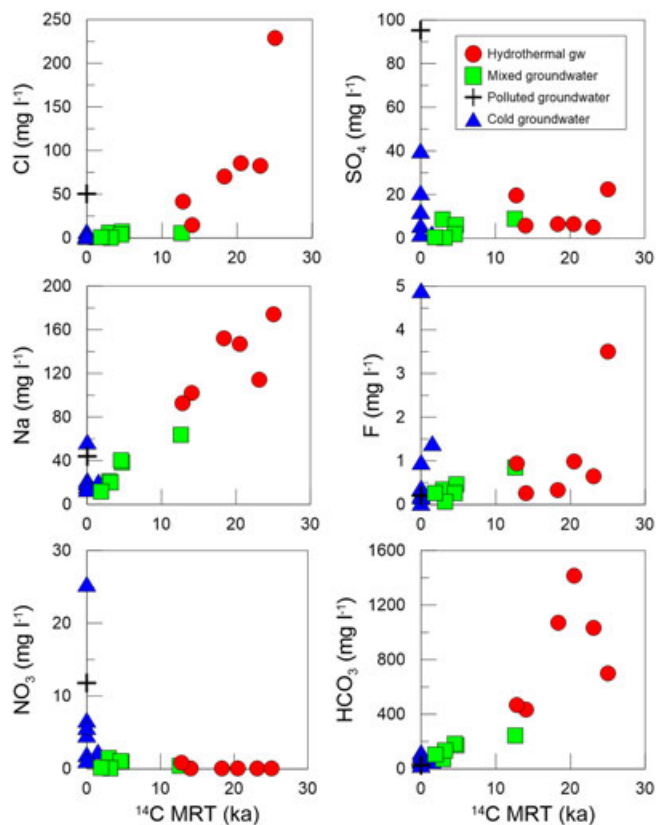


FIGURE 8 Radiocarbon and chlorofluorocarbons (CFCs) correlating to residence times vs. selected chemical elements

Nextipac, La Venta del Astillero). Their locations indicate that NO_3 inputs are derived partly from the urban drainage system and partly from the use of fertilizers. Much of this increase in NO_3 concentration

has occurred during the past few decades, reaching $\text{NO}_3\text{-N}$ values of up to 25 mg/L. These increased NO_3 values are expected to persist over the next few decades, regardless of whether NO_3 pollution continues, because the microbial reduction of NO_3 is precluded at the measured DO contents of 3 to 8 mg/L. However, the previously described mixing of groundwater between the upper and lower aquifers may mitigate the effects of this contamination, except in recharge areas.

Sulfate concentrations appear to follow two different trends: First, young waters contain elevated concentrations of up to 95 mg/L, which can likely be attributed to surface sources such as ammonium sulfate fertilizers; second, hydrothermal waters also contain elevated concentrations, thus reflecting a geothermal influence. Bicarbonate patterns are similar to those of Na and record relatively high concentrations in hydrothermal waters compared to other waters. Alkali and alkaline earth metals, Cl, and HCO_3 tend to increase with groundwater age due to water–rock interactions (Figure 7; Tables 1 and 2). Strontium isotopes ($^{87}\text{Sr}/^{86}\text{Sr}$ ratio) measured in water can be used to characterize sources and processes responsible for elevated concentrations of SO_4 and other groundwater constituents (Horst et al., 2011).

Fluoride concentrations above the drinking water standard have been detected in cold and hydrothermal waters in several communities (San Juan de Ocotlán, San Sebastián El Grande, Santa Anita, Los Gavilanes, La Tijera, El Palomar, south Zapopan, and west Tlaquepaque), which supports the findings of a previous study (Sánchez-Díaz, 2007). In general, fluorite and hydroxyl minerals such as muscovite, biotite, and apatite may be the source of this F. Biotite is a common accessory mineral in igneous rocks within the study area (Morán-Ramírez et al., 2016). Cold waters with elevated HCO_3 and Na contents are alkaline and have relatively high concentrations of

hydroxyl ions, which can replace F in fluoride-bearing materials and release F into the groundwater (Guo, Wang, Gao, & Ma, 2007).

The high values of F in hydrothermal waters indicate the presence of an additional source of F, such the process of evaporation. In general, a solubility control on calcium fluoride (CaF_2) produces an inverse relationship between Ca and F ions. After evaporation, calcite is precipitated, which reduces the concentration of Ca and consequently enriches the concentration of F in the remaining groundwater. In the Guadalajara aquifer system, only hydrothermal waters are oversaturated with calcite, possibly due to evaporation, and the precipitation of calcite may thus promote the dissolution of calcium fluoride, as has been previously suggested by Morán-Ramírez et al. (2016).

In the cold and polluted groundwater samples, there is a general correlation between SO_4 and NO_3 ($r^2 = .7$, $p = .01$), but not between Cl and NO_3 ($r^2 = .0$; $p = .90$); an anticorrelation exists between F and NO_3 ($r^2 = .2$; $p = .43$). These data suggest that, in most cases, fertilizer (rather than human or animal waste) may represent the source of NO_3 in these sample, thus confirming that F and NO_3 have distinct sources. Nitrate isotopes could be used to test this hypothesis (Pastén-Zapata, Ledesma-Ruiz, Harter, Ramírez, & Mahlknecht, 2014).

The map of CFC-12 concentrations in Figure 7 indicates a degree of vulnerability to surface sources of contamination. A trend can be observed in which sites with higher CFC concentrations have greater expected contributions from vertical surface sources. This distribution suggests that the Atemajac aquifer system, which includes much of the GMA, is highly vulnerable to surface contamination. The Toluquilla aquifer system records relatively low vulnerability, with the exception of those sites located near the La Primavera Caldera. This interpretation is consistent with the pattern of recharge outlined above and is supported by the distribution of measured NO_3 concentrations in the study area. Unfortunately, due to the limited number and inadequate spatial distribution of samples in this study, our ability to assess intrinsic vulnerability is limited. For instance, the eastern part of the study area is not sufficiently covered by sampling sites. However, it is expected that groundwater vulnerability increases towards the Santiago River.

6 | SUMMARY AND CONCLUSIONS

Natural and anthropogenic processes have impaired the groundwater quality of the aquifer system that underlies and provides water to the GMA. Faults in this complex neotectonic environment facilitate the vertical upward movement of hydrothermal fluids from the magma chamber below the La Primavera Caldera. These fluids mix with regional groundwater in the lower aquifer unit and local groundwater in the upper aquifer unit. This groundwater is also polluted by urban wastewater sewage and agricultural irrigation cycling. In this study, several elements of interest (i.e., chloride, nitrate, sulfate, and fluoride) were investigated in detail in relation to groundwater flow patterns.

Local groundwater is formed primarily by the infiltration of rainfall over the La Primavera Caldera in the central western region of the study area, followed by the variable influence of evaporation. Groundwater flows to the northeast in the Atemajac Valley and to the southeast in the Toluquilla Valley, before discharging into the Santiago River.

Groundwater from recharge zones is of the Na-HCO_3 type and records little mixing. In contrast, groundwater from nonrecharge zones is of the Mg-HCO_3 and mixed- HCO_3 type, which records mixing with prebomb waters, and the Na-SO_4 to mixed HCO_3 type, which records urban anthropogenic pollution.

This mixing phenomenon is mainly caused by bore leakages. Geochemical models indicate that the contribution of hydrothermal waters reaches a maximum of 0.5% in the upper aquifer portion of the Atemajac Valley and a maximum of 20% in the upper aquifer portion of the Toluquilla Valley. Radiocarbon age dating reveals that groundwater from recharge zones is generally modern, whereas the age of groundwater from nonrecharge zones varies from zero age to 27 ka. Although the spatial distribution of CFC concentrations correlates with those of tritium and radiocarbon, these tracers may not produce reliable age estimates due to evaporation effects and uncertain lag times in the thick unsaturated zone. Additionally, several sites in urbanized and industrialized areas are contaminated, which makes it impossible to determine ages.

Elevated nitrate levels in groundwater are mostly concentrated in or near recharge zones in the western region of the study area. These inputs come from urban drainage systems and fertilizer use over the past several decades. Nitrate levels are expected to continue increasing in the future, regardless of whether nitrate pollution is controlled. Sulfate contamination originates from two different sources: ammonium sulfate fertilizers in cold groundwater and mixing with hydrothermal fluids in other waters. Fluoride contamination is most likely caused by fluorite-containing minerals such as biotite. A secondary potential source is that of fluoride-bearing minerals exchanging fluoride with hydroxyl ions on their surfaces. It is also likely that calcium fluoride controls fluoride concentrations in hydrothermal waters.

We recommend that a more detailed investigation be performed to study contamination on a local level. Strontium and sulfate isotopes may assist in identifying and characterizing the sources and processes responsible for elevated sulfate concentrations, and analyses of nitrate isotopes and halogens may improve our understanding of the sources and processes responsible for elevated nitrate concentrations. The upper groundwater system is vulnerable to surface sources of contamination, and the upper aquifer region below the Atemajac Valley and most of the GMA is more vulnerable than the region located below the western Toluquilla Valley. Therefore, it is imperative to protect the groundwater sources in and near recharge areas, to develop additional studies to delimit priority areas for groundwater protection and an effective water table, and to establish a water quality monitoring program. These activities should be used to help formulate management policies, such as the protection of recharge zones, adaptation of permits, and control of water extraction. Supplementary Information describes with more detail the recommendations for groundwater protection and management.

ACKNOWLEDGMENTS

This work was financially supported by Fundación FEMSA and the Chair for Water Science and Technology (Tecnológico de Monterrey). Fundación FEMSA had no role in the study design, data collection and analysis, decision to publish, or preparation of the manuscript.

We would like to thank A. Mazón for technical assistance in the field. The observations of the reviewers helped to greatly improve the quality of the manuscript.

REFERENCES

- APHA (American Public Health Association) (2012). *Standard methods for the examination of water and wastewater*. Washington, DC: Theclassics US.
- Appelo, C. A. J., & Postma, D. (2005). Ion exchange. In C. Appelo, & D. Postma (Eds.), *Geochemistry, groundwater and pollution* (pp. 241–309). Leiden, Netherlands: Balkema Publishers.
- Araguás-Araguás, L., & Gonfiantini, R. (1993). Isotopic patterns in modern global precipitation. In P. K. Swart, K. C. Lohmann, J. Mckenzie, & S. Savin (Eds.), *Climate change in continental isotopic records. Geophysical Monograph 78* (pp. 1–36). Washington D.C.: American Geophysical Union.
- Böhlke, J. K., Jurgens, B. C., Uselmann, D. J., & Eberts, S. M. (2014). Educational webtool illustrating groundwater age effects on contaminant trends in wells. *Groundwater*, *52*, 8–9.
- Broers, H. P. (2004). The spatial distribution of groundwater age for different geohydrological situations in the Netherlands: Implications for groundwater quality monitoring at the regional scale. *Journal of Hydrology*, *299*, 84–106.
- Campos-Enríquez, J. O., Domínguez-Méndez, F., Lozada-Zumaeta, M., Morales-Rodríguez, H. F., & Andaverde-Arredondo, J. A. (2005). Application of the Gauss theorem to the study of silicic calderas: The calderas of La Primavera, Los Azufres, and Los Humeros (Mexico). *Journal of Volcanology and Geothermal Research*, *147*, 39–67.
- Cartwright, I., & Morgenstern, U. (2012). Constraining groundwater recharge and the rate of geochemical processes using tritium and major ion geochemistry: Ovens catchment, southeast Australia. *Journal of Hydrology*, *475*, 137–149.
- Clark, I. D., & Fritz, P. (1997). *Environmental isotopes in hydrogeology*. New York, NY: Lewis Publishers.
- CONAGUA (Comisión Nacional del Agua). (2009). Determinación de la Disponibilidad de Agua en el Acuífero Toluquilla, Estado de Jalisco [Determination of water availability in the Toluquilla aquifer, Jalisco state]. Mexico City, Mexico.
- CONAGUA (Comisión Nacional del Agua). (2015a). Actualización de la disponibilidad media anual de agua en el acuífero Atemajac (1401), Estado de Jalisco [Actualization of average annual water availability in the Atemajac aquifer (1401), Jalisco State]. Mexico City, Mexico. Internet: http://www.gob.mx/cms/uploads/attachment/file/103711/DR_1401.pdf (18/03/2017)
- CONAGUA (Comisión Nacional del Agua). (2015b). Actualización de la disponibilidad media anual de agua en el acuífero Toluquilla (1402), Estado de Jalisco [Actualization of average annual water availability in the Toluquilla aquifer (1402), Jalisco State]. Mexico City, Mexico. Internet: http://www.gob.mx/cms/uploads/attachment/file/103712/DR_1402.pdf (18/03/2017)
- Cook, P. G., & Solomon, D. K. (1995). Transport of atmospheric trace gases to the water table: Implications for groundwater dating with chlorofluorocarbons and Krypton 85. *Water Resources Research*, *31*, 263–270.
- Cook, P. G., & Solomon, D. K. (1997). Recent advances in dating young groundwater: Chlorofluorocarbons, and 85Kr. *Journal of Hydrology*, *191*, 245–265.
- Darling, W. G., Morris, B., Stuart, M. E., & Goody, D. C. (2005). Groundwater age indicators from public supplies tapping the chalk aquifer of southern England. *Water and Environment Journal*, *19*, 30–40.
- Deines, P., Langmuir, D., & Harmon, R. S. (1974). Stable carbon isotope ratios and the existence of a gas phase in the evolution of carbonate ground waters. *Geochimica et Cosmochimica Acta*, *38*, 1147–1164.
- Demant, A. (1978). Características del Eje Neovolcánico Transmexicano y sus problemas de interpretación [Characteristics of the trans-Mexican Neovolcanic Belt and its problems of interpretation]. *Revista Mexicana de Ciencias Geológicas*, *2*, 172–187.
- Eastoe, C. J., Watts, C. J., Ploughe, M., & Wright, W. E. (2012). Future use of tritium in mapping pre-bomb groundwater volumes. *Ground Water*, *50*, 87–93.
- Eberts, S. M., Böhlke, J. K., Kauffman, L. J., & Jurgens, B. C. (2012). Comparison of particle-tracking and lumped-parameter age-distribution models for evaluating vulnerability of production wells to contamination. *Hydrogeology Journal*, *20*, 263–282.
- Engesgaard, P., Hojberg, A. L., Hinsby, K., Jensen, K. H., Laier, T., Larsen, F., & Plummer, & L. N. (2004). Transport and time lag of chlorofluorocarbon gases in the unsaturated zone, Rabis Creek, Denmark. *Vadose Zone Journal*, *3*, 1249–1261.
- Fontes, J.-C., & Garnier, J.-M. (1979). Determination of the initial 14 C activity of the total dissolved carbon: A review of the existing models and a new approach. *Water Resources Research*, *15*, 399–413.
- Guo, Q., Wang, Y., Gao, X., & Ma, T. (2007). A new model (DRARCH) for assessing groundwater vulnerability to arsenic contamination at basin scale: A case study in Taiyuan basin, northern China. *Environmental Geology*, *52*, 923–932.
- Gutiérrez-Negrin, L. (1988). La Primavera, Jalisco, Mexico: Geothermal field. *Transactions of the Geothermal Research Council*, *12*, 161–165.
- Gutiérrez-Negrin, L. (1991). Recursos geotérmicos en La Primavera, Jalisco, Mexico [Geothermal resources in La Primavera]. *Ciencia y Desarrollo*, *16*, 57–69.
- Harvey, C. F., Ashfaq, K. N., Yu, W., Badruzzaman, A. B. M., Ali, M. A., Oates, P. M., & Ahmed, M. F. (2006). Groundwater dynamics and arsenic contamination in Bangladesh. *Chemical Geology*, *228*, 112–136.
- Hernández-Antonio, A., Mahlknecht, J., Tamez-Meléndez, C., Ramos-Leal, J., Ramírez-Orozco, A., Parra, R., & Eastoe, C. J. (2015). Groundwater flow processes and mixing in active volcanic systems: The case of Guadalajara (Mexico). *Hydrology and Earth System Sciences*, *19*, 3937–3950.
- Horst, A., Mahlknecht, J., López-Zavala, M. A., & Mayer, B. (2011). The origin of salinity and sulphate contamination of groundwater in the Colima State, Mexico, constrained by stable isotopes. *Environmental Earth Sciences*, *64*, 1931–1941.
- Horst, A., Mahlknecht, J., & Merkel, B. J. (2007). Estimating groundwater mixing and origin in an overexploited aquifer in Guanajuato, Mexico, using stable isotopes (strontium-87, carbon-13, deuterium and oxygen-18). *Isotopes in Environmental and Health Studies*, *43*, 323–338.
- Horst, A., Mahlknecht, J., Merkel, B. J., Aravena, R., & Ramos-Arroyo, Y. R. (2008). Evaluation of the recharge processes and impacts of irrigation on groundwater using CFCs and radiogenic isotopes in the Silao-Romita basin, Mexico. *Hydrogeology Journal*, *16*, 1601–1614.
- IMTA (Instituto Mexicano de Tecnología del Agua). (1992). Estudio isotópico e hidroquímico de los acuíferos de Toluquilla-Ocotlán-La Barca, en el Estado de Jalisco [Isotopic and hydrochemical study of the Toluquilla-Ocotlán-La Barca aquifers, in the State of Jalisco]. Technical report. Jiutepec, Morelos, México.
- Ingerson, E., & Pearson, F. J. (1964). Estimation of age and rate of motion of groundwater by the 14C-method. In Y. Miyake, & T. Koyama (Eds.), *Recent researches in the fields of atmosphere, hydrosphere and nuclear geochemistry* (pp. 263–283). Tokyo, Japan: Maruzen.
- Jurgens, B. C., Böhlke, J. K., & Eberts, S. M. (2012). TracerLPM (Version 1): An excel® workbook for interpreting groundwater age distributions from environmental tracer data, United States Geological Survey Techniques and Methods Report 4-F3, 60.
- Jurgens, B. C., Böhlke, J. K., Kauffman, L. J., Belitz, K., & Esser, B. K. (2016). A partial exponential lumped parameter model to evaluate groundwater age distributions and nitrate trends in long-screened wells. *Journal of Hydrology*, *543*, 109–126.
- Kalin, R. M. (2000). Radiocarbon dating of groundwater systems. In P. Cook, & A. L. Herczeg (Eds.), *Environmental tracers in subsurface hydrology* (pp. 111–144). Dordrecht: Kluwer Academic.
- Kauffman, L. J., Baehr, A. L., Ayers, M. A., & Stackelberg, P. E. (2001). Effects of land use and travel time on the distribution of nitrate in the Kirkwood-Cohansey aquifer system in southern New Jersey. *US Geol Surv Sci Invest Rep 01-4117*, 49

- Kazemi, G. A., Lehr, J. H., & Perrochet, P. (2006). *Groundwater age*. Hoboken, NJ: Wiley.
- Kendall, C., & McDonnell, J. J. (2012). *Isotope tracers in catchment hydrology*. Amsterdam, Netherlands: Elsevier Science.
- Laaksoharju, M., Skårman, E., Gómez, J. B., & Gurban, I. (2009). *M3 version 3: User's manual SKB TR-09-09*. Sweden: Svensk Kärnbränslehantering AB.
- Leibundgut, C., Maloszewski, P., & Külls, C. (2009). *Tracers in hydrology*. West Sussex, UK: Wiley.
- Li, H., & Jiao, J. J. (2005). One-dimensional airflow in unsaturated zone induced by periodic water table fluctuation. *Water Resources Research*, 41, W04007.
- Li, J., Pang, Z., Froehlich, K., Huang, T., Kong, Y., Song, W., & Yun, H. (2015). Paleo-environment from isotopes and hydrochemistry of groundwater in East Junggar Basin, Northwest China. *Journal of Hydrology*, 529, 650–661.
- Maciel-Flores, R., & Rosas-Elguera, J. (1992). Modelo geológico y evaluación del campo geotérmico La Primavera, Jal., México [Geological model and evaluation of the geothermal field La Primavera]. *Geofísica Internacional*, 31, 359–370.
- Mahlknecht, J., Gárfias-Solis, J., Aravena, R., & Tesch, R. (2006a). Geochemical and isotopic investigations on groundwater residence time and flow in the Independence Basin, Mexico. *Journal of Hydrology*, 324, 283–300.
- Mahlknecht, J., Horst, A., Hernández-Limón, G., & Aravena, R. (2008). Groundwater geochemistry of the Chihuahua city region in the Rio Conchos basin (northern Mexico) and implications for water resources management. *Hydrological Processes*, 22, 4736–4751.
- Mahlknecht, J., Medina-Mejía, M. G., Gárfias-Solis, J., & Cano-Aguilera, I. (2006b). Intrinsic aquifer vulnerability assessment: Validation by environmental tracers in San Miguel de Allende, Mexico. *Environmental Geology*, 51, 477–491.
- Mahlknecht, J. R., Schneider, J. F., Merkel, B. J., de Leon, I., & Bernasconi, S. M. (2004). Groundwater recharge in a sedimentary basin in semi-arid Mexico. *Hydrogeology Journal*, 12, 511–530.
- Mahood, G. A. (1980). Geological evolution of a pleistocene rhyolitic center—Sierra La Primavera, Jalisco, México. *Journal of Volcanology and Geothermal Research*, 8, 199–230.
- Mahood, G. A. (1981). A summary of the geology and petrology of the Sierra La Primavera, Jalisco, Mexico. *Journal of Geophysical Research*, 86, 10137–10152.
- Małoszewski, P., & Zuber, A. (1982). Determining the turnover time of groundwater systems with the aid of environmental tracers: 1. Models and their applicability. *Journal of Hydrology*, 57, 207–231.
- Maloszewski, P., & Zuber, A. (1996). Lumped parameter models for the interpretation of environmental tracer data. In *Manual on mathematical models in isotope hydrology (IAEA-TECDOC-910)* (pp. 9–58). Vienna, Austria: IAEA.
- McCrea, J. M. (1950). On the isotopic chemistry of carbonates and a paleotemperature scale. *The Journal of Chemical Physics*, 18, 849–857.
- McMahon, P. B., Böhlke, J. K., Kauffman, L. J., Kipp, K. L., Landon, M. K., Crandall, C. A., & Brown, C. J. (2008). Source and transport controls on the movement of nitrate to public supply wells in selected principal aquifers of the United States. *Water Resources Research*, 44, W04401.
- Mook, W. G., Bommerson, J. C., & Staverman, W. H. (1974). Carbon isotope fractionation between dissolved bicarbonate and gaseous carbon dioxide. *Earth and Planetary Science Letters*, 22, 169–176.
- Morán-Ramírez, J., Ledesma-Ruiz, R., Mahlknecht, J., & Ramos-Leal, J. A. (2016). Rock–water interactions and pollution processes in the volcanic aquifer system of Guadalajara, Mexico, using inverse geochemical modeling. *Applied Geochemistry*, 68, 79–94.
- Morgenstern, U., & Daughney, C. J. (2012). Groundwater age for identification of baseline groundwater quality and impacts of land-use intensification—The national groundwater monitoring programme of New Zealand. *Journal of Hydrology*, 456–457, 79–93.
- Morgenstern, U., Daughney, C. J., Leonard, G., Gordon, D., Donath, F. M., & Reeves, R. (2015). Using groundwater age and hydrochemistry to understand sources and dynamics of nutrient contamination through the catchment into Lake Rotorua, New Zealand. *Hydrology and Earth System Sciences*, 19, 803–822.
- Morris, B., Stuart, M. E., Darling, W. G., & Goody, D. C. (2005). Use of groundwater age indicators in risk assessment to aid water supply operational planning. *Water and Environment Journal*, 19, 41–48.
- Newman, B. D., Osenbrück, K., Aeschbach-Hertig, W., Solomon, D. K., Cook, P., Rózański, K., & Kipfer, R. (2010). Dating of 'young' groundwaters using environmental tracers: Advantages, applications, and research needs. *Isotopes in Environmental and Health Studies*, 46, 259–278.
- Nilson, R. H., Peterson, E. W., Lie, K. H., Burkhard, N. R., & Hearst, J. R. (1991). Atmospheric pumping: A mechanism causing vertical transport of contaminated gases through fractured permeable media. *Journal of Geophysical Research*, 96, 21933–21948.
- Oestlund, H. G., & Werner, E. (1962). The electrolytic enrichment of tritium and deuterium for natural tritium measurements. In *tritium in the physical and biological sciences*. v. 1. Proceedings of a symposium.
- Oster, H., Sonntag, C., & Münnich, K. O. (1996). Groundwater age dating with chlorofluorocarbons. *Water Resources Research*, 32, 2989–3001.
- Parkhurst, D. L., & Charlton, S. R. (2008). Netpathxl—An excel interface to the program NETPATH. U.S. Geological Survey Techniques and Methods 6-A26.
- Pastén-Zapata, E., Ledesma-Ruiz, R., Harter, T., Ramírez, A. I., & Mahlknecht, J. (2014). Assessment of sources and fate of nitrate in shallow groundwater of an agricultural area by using a multi-tracer approach. *Science of the Total Environment*, 470–471, 855–864.
- Plummer, L. N., Busenberg, E., Böhlke, J. K., Nelms, D. L., Michel, R. L., & Schlosser, P. (2001). Groundwater residence times in Shenandoah National Park, Blue Ridge Mountains, Virginia, USA: A multi-tracer approach. *Chemical Geology*, 179, 93–111.
- Plummer, L. N., Busenberg, E., & Cook, P. G. (2006). Principles of chlorofluorocarbon dating. In L. N. Plummer, E. Busenberg, & P. G. Cook (Eds.), *Use of chlorofluorocarbons in hydrology a guidebook* (pp. 17–29). Vienna, Austria: International Atomic Energy Agency.
- Plummer, L. N., Busenberg, E., Drenkard, S., Schlosser, P., Ekwurzel, B., Weppernig, R., & Michel, R. L. (1998). Flow of river water into a karstic limestone aquifer—2. Dating the young fraction in groundwater mixtures in the Upper Floridan aquifer near Valdosta, Georgia. *Applied Geochemistry*, 13, 1017–1043.
- Plummer, L. N., Busenberg, E., Eberts, S. M., Bexfield, L. M., Brown, C. J., Fahlgvist, L. S., & Landon, M. K. (2008). Low-level detections of halogenated volatile organic compounds in groundwater: Use in vulnerability assessments. *Journal of Hydrologic Engineering*, 13, 1049–1068.
- Plummer, L. N., & Glynn, P. D. (2013). *Radiocarbon dating in groundwater systems isotope methods for dating old groundwater*. Vienna, Austria: International Atomic Energy Agency.
- Plummer, L. N., Prestemon, E. C., & Parkhurst, D. L. (1991). An interactive code (NETPATH) for modelling net geochemical reactions along a flow path. United States Geological Survey Water-Resources Investigations Report 91–4078.
- Plummer, N., Prestemon, E. C., & Parkhurst, D. L. (1994). An interactive code (NETPATH) for modeling NET geochemical reactions along a flow PATH. Geological Survey Water Resources Investigations Report, 94–4169. US Geological Survey.
- Ramírez, S. G., del Razo, J., & Mata, V. V. M. (1982). Hidrología regional de la zona geotérmica de la Primavera-San Marcos-Hervores de la Vega, Jalisco [Regional hydrology of La Primavera-San Marcos-Hervores de la Vega geothermal zone, Jalisco]. Technical Report. Comisión Federal de Electricidad, Mexico City.
- Sánchez-Díaz, L. F. (2007). Origen, transporte, distribución y concentraciones de los fluoruros en el sistema hidrogeológico volcánico Atemajac-Toluquilla, Jalisco [Origin, transport, distribution and concentrations of fluorides in the hydrogeological volcanic system of

- Atemajac-Toluquilla, Jalisco] (Ph.D. dissertation). Instituto de Geofísica, Universidad Nacional Autónoma de México, Mexico City, Mexico.
- SIAPA (Sistema Intermunicipal de Agua Potable y Alcantarillado). (2004). Estudio geohidrológico Atemajac-Toluquilla [Geohydrologic study of Atemajac-Toluquilla]. Elaborated by Geología y Exploraciones SA. Guadalajara, Jalisco, México.
- Stewart, M. K., Morgenstern, U., & McDonnell, J. J. (2010). Truncation of stream residence time: How the use of stable isotopes has skewed our concept of streamwater age and origin. *Hydrological Processes*, 24, 1646–1659.
- Stewart, M. K., Morgenstern, U., McDonnell, J. J., & Pfister, L. (2012). The 'hidden streamflow' challenge in catchment hydrology: A call to action for stream water transit time analysis. *Hydrological Processes*, 26, 2061–2066.
- Turnadge, C., & Smerdon, B. D. (2014). A review of methods for modelling environmental tracers in groundwater: Advantages of tracer concentration simulation. *Journal of Hydrology*, 519, 3674–3689.
- Urrutia-Fucugauchi, J., Alva-Valdivia, L. M., Rosas-Elguera, J., Campos-Enriquez, O., Goguitchaichvili, A., Soler-Arechalde, A. M., & Sánchez-Reyes, S. (2000). Magnetostratigraphy of the volcanic sequence of Río Grande de Santiago-Sierra de la Primavera region, Jalisco, western Mexico. *Geofísica Internacional*, 39, 247–265.
- USGS (United States Geological Services). (2015). The Reston groundwater laboratory. The CFC air curves. Internet: https://water.usgs.gov/lab/software/air_curve/index.html (10/11/2015)
- Venegas, S. S., Ramírez, S. G., Romero, G. C., Reyes, V. P., Razo, M. A., Gutiérrez-Negrín, L. C. A., Arellano, G. F., & Rerezera, Z. J. (1991). La Primavera geothermal field, Jalisco In *The Geology of North America*, G. P. Salas (Ed.), *Economic Geology, Mexico* (pp. 95–106). Boulder, CO: The Geological Society of America.
- Vogel, J. C. (1970). ^{14}C dating of groundwater. IAEA (Ed.), In *Isotope hydrology* (pp. 225–237). Vienna, Austria: IAEA.
- Vogel, J. C., Grootes, P. M., & Mook, W. G. (1970). Isotopic fractionation between gaseous and dissolved carbon dioxide. *Zeitschrift für Physik a Hadrons and Nuclei*, 230, 225–238.
- Wassenaar, L. I., Van Wilgenburg, S. L., Larson, K., & Hobson, K. A. (2009). A groundwater isoscape (δD , $\delta^{18}\text{O}$) for Mexico. *Journal of Geochemical Exploration*, 102, 123–136.
- Zárate-del-Valle, P. F., Ramírez-Sánchez, H. U., Fernex, F., Simoneit, B. R., & Israde-Alcántara, I. (2011). Radiocarbon age inversions and progression: Source and causes in Late Holocene sediments from Lake Chapala, western Mexico. *Environmental Earth Sciences*, 63(5), 1011–1019.
- Zuber, A. (1986). Mathematical models for the interpretation of environmental radioisotopes in groundwater systems. In P. Fritz, & J. Fontes (Eds.), *Handbook of environmental isotope geochemistry* (Vol. 2) *the terrestrial environment B* (pp. 1–59). New York, NY: Elsevier.
- Zuber, A., Witczak, S., Rózański, K., Śliwka, I., Opoka, M., Mochalski, P., & Duliński, M. (2005). Groundwater dating with ^3H and SF_6 in relation to mixing patterns, transport modelling and hydrochemistry. *Hydrological Processes*, 19, 2247–2275.

SUPPORTING INFORMATION

Additional Supporting Information may be found online in the supporting information tab for this article.

How to cite this article: Mahlknecht J, Hernández-Antonio A, Eastoe CJ, et al. Understanding the dynamics and contamination of an urban aquifer system using groundwater age (^{14}C , ^3H , CFCs) and chemistry. *Hydrological Processes*. 2017;31:2365–2380. <https://doi.org/10.1002/hyp.11182>